Pulse modulation by switches of high frequency of alternating current circuits and application of this method

MARCIS PRIEDITIS, IVARS RANKIS, AGRIS TREIMANIS
Institute of IEEI
Riga Technical University
Liepaja, Liedaga iela 3
LATVIJA

Abstract: - This paper is devoted to analysis of AC pulse modulation systems and calculation method explanation for such systems. Analysis of load filter parameters are performed by regressive estimation of filtering system parameters. The utility of such system has been reviewed in the context of the application of 3-phase induction motor.

Key-Words: - pulse modulation; AC; motor control; filtering; regressive estimation; unipolar modulation.

1 Introduction

Evaluating the available publications on the regulation of processes in DC and AC circuits [1], one can observe that in the main research, there are devices with elements and circuits of DC current. In this case, the regulation of processes is performed by the method of pulse regulation using pulse-width modulation PWM and switching device frequencies up to the several hundred kilohertz [1-5]. Devices with alternating current circuits are either supplied with intermediate circuits and DC nodes in which high-frequency pulse regulation is carried out, or controlled by electronic devices operating at the frequency of the supplying alternating current, i.e., the method of changing the duration of current flow through the circuit during each half-period of the supplying alternating current is used. In this case, single-position controlled semiconductor elements - thyristors or triacs, controlled only by the moment of switching, are used. Controllability is achieved by changing the unlocking interval in the half-cycle of the supply AC voltage, i.e., the pulse-phase method of AC regulation is used [6, 7]. Many theoretical studies have been devoted to the development and study of such control systems for processes in alternating current circuits [1]. As a result, many practically applied systems and devices have been created [1, 8].

The use of the pulse-phase method of AC regulation leads to a significant deterioration in the quality of power supply as well as in load. Firstly, the waveform of the currents in both nodes is far from sinusoidal, which is reflected in the increased values of the harmonic current distortion indicators of the circuits under current conductivity and the current distortion indicator $I_v = I(1)/I$. Ш. Secondly, the method itself is based on the introduction of a forced phase shift between fundamental waves of currents and supply voltages, which is reflected in low values of the $\cos\phi(1)$ of the shift angle $\phi(1)$ of the fundamental harmonic current relative to the supply alternating current wave. As a result, the power factor - the ratio of the real power P and the apparent power S, defined as the product of the multiplication of I_v and $\cos\phi(1)$ which is evaluated to obtain small values, i.e., the power quality is poor. The indicated disadvantages - strong distortion of the current shape and forced shift of the fundamental current wave are not easy surmountable, which means that there are no great opportunities to improve the state in the direction of improving the power quality without extra hardware.

Considering the successful and multifunctional application of pulse regulation of DC circuits [9], it could be assumed that effective use of this method of current regulation is also possible to be applied in AC circuits, either. Of course, all electronic switches used in AC circuits must be of alternating current, i.e., allow carrying out regulation regardless of the direction of the current at the moment of switching the AC circuit. This requirement of course complicates the realization of AC switches. Basically, technical solutions are reduced either to the creation of circuits with two series-connected transistors of opposite polarity of conductivity [10] or to the inclusion in the diagonal of a single-phase diode bridge of one commutable transistor [11]. The use of transistor alternating current switches allows high-frequency modulation of processes in the AC circuits, which in turn allows synthesizing both new

fundamental waves of alternating voltages of system elements and currents of the same type. The use of transistor alternating current switches allows high-frequency modulation of processes in the AC circuits, which in turn allows, moreover, these fundamental waves of electrical signals can be both with an adjustable amplitude and an adjustable phase shift with respect to the voltage (current) wave.

At present, AC systems with high-frequency modulated switches in the scientific and technical literature aspects, have not been concerned enough. Therefore, there is no great clarity both with the use of methods of analysis and calculation of processes, and with multifunctional application. Taking into account the possibility of generating new fundamental waves of voltages and currents, the analysis can be built on the basis of generating the effective (RMS) values of modulated currents and voltages considering their interphase shifts, i.e., use the method of vector analysis, as shown in [12]. However, for a reasonable application of the method, it is necessary to accumulate many verified analyzed solutions, which seems to be the purpose of this research work. Offering filter parameter assessment methods could give great benefit in other applications [13, 14] as well as they could be used on smart grid development technologies [15].

2 Algorithm of unipolar modulation of alternating current

The load with this method during one period of modulation Tm (electronic state on-off) is connected periodically during the half-period of the supplying alternating current u1 to the same pole of the supply voltage, but during the off-interval of the switch the load voltage is at the zero level (i.e. load is shortened). To the load during the half-period of the supply voltage, there are two values u1 and 0 across the load. For this, in each half-cycle, two states should be used, one connects the load to the source, and the other shortens the voltage of the load (see the schematic in Fig. 1).

In the circuit Fig. 1, it is possible to obtain a modulated fundamental harmonic of the load voltage in a directly proportional (concurrent) form with respect to the supply voltage wave, and in an inverted form. For the first, one of the switches of the direct connecting circuit S1/S2 must always be turned on over half-cycle of supply voltage. To implement the second option, one switch must always be turned on in the reverse circuit S4, S3. For example, to implement the first option, that is the switch S2, but switch S1 is providing on-duty operation D_{con}; to

implement the second – the switch S3 could stay constantly turned-on, but switch S4 provides on-duty operation D_R for the second option. Zeroing of the load voltage is performed through a permanently switched on switch from one circuit and a complementary (1-D) modulated switch of another switch control circuit. For example, in the coordinated control mode, when S1 is locked, and S2 remains permanently on, $(1-D)_{con}$ interval is carried out through S3, which complements the S1. Thus, for coordinated control mode D_{con} corresponds to S1 and S2, and $(1-D)_{con}$ corresponds to S2 and S3. In the reverse case of control D_R corresponds to S4 and S3, and $(1-D)_R$ – to the mode S4 and S2. The latter is complementary to the S4 switch.
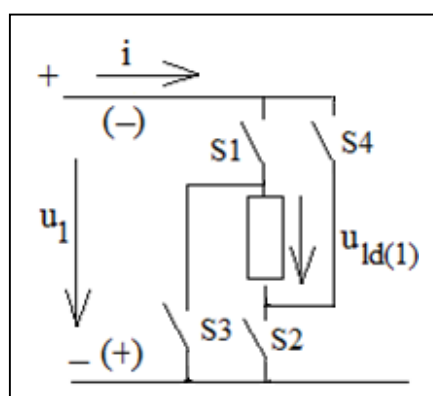

Fig. 1. Scheme for direct proportional (concurrent con) and inverse I proportional modulation of the load voltage.

To balance the loads on the switches, when the polarity of the supply voltage is reversed, the connection can be made to the other pole of the supply voltage. Thus, two more switches are required to implement the second half cycle. Later, as appear in Figure 1, switches S1 and S3 carry out control at the one polarity of the supply voltage, switches S2 and S4 – performing control in opposite polarity of the voltage of one-phase alternating supply voltage. If the supply voltage is also negative, switch S2 is performing the modulation (D interval), whilst S1 staying constantly on, and the load is short-circuited with the switches S4 (see the switching table).

Table I   Switching table.

nl	>0			<0		
uld(1)	>0	0	<0	>0	0	<0
S1	on	off	off	on	on	on
S2	on	on	on	off	off	on
S3	off	on	on	on	off	Off
S4	off	off	on	on	on	Off
	D	1-D			1-D	D

The fundamental harmonic of the modulated load voltage could be described as:

$$u_{ld(1)} = D \cdot U_{1m} sin\omega t \qquad (1)$$

where $D \cdot U_{1m}$ is the amplitude of the fundamental, and dividing this indicator by $\sqrt{2}$ is the RMS value of the fundamental.

Examples of load voltage diagrams for various options are shown in Fig. 2. In the first case, where both voltages coincide in polarity at the conditionally positive polarity of supply voltage, the S1 switch performs the direct modulation function D_{con}(duty) by periodically connecting the load to the power source, while the S3 switch constantly turned-on and switch S2 implements the zero off-duty pause (1-D)$_{con}$. If the polarity of the supply voltage has switched to be negative, the function D_{con} is performed by the S2 switch and (1-D)$_{con}$ – the S4 switch.

In the case when both voltages – supply and load – have conditionally opposite signs whereas the supply voltage has a positive polarity, the D_R and (1-D)$_R$ functions are performed by the S4 switch and S2 switches (but at the same time S3 remains constantly on), respectively. In the fourth version of the algorithms, when, with different polarities, the supply voltage has a conditionally negative sign the interval D is carried out with the switch S3, but 1-D with S1 (but with constantly on S4 switch). As a result, for the implementation of all four algorithms, a special block for control of the polarity of the supply and load voltages is needed and a logical node is required to select one of the four algorithms.

From the obtained diagrams, it is possible to determine the effective and amplitude values of the voltages of the circuit elements (see the data table II).

As it can be observed from calculations and experiments, amplitude meanings are well complying, but RMS meanings measured with voltmeter are different as it was correctly found from the results of Fourier transformation. Due to lack of voltmeters, measuring the RMS values of fundamental waves it should be difficult to use measured vectors but only calculated could be admissible with certain accuracy. The problem initiates at operation with modulated signals, while RMS meanings are far from estimated by diagrams of voltages.
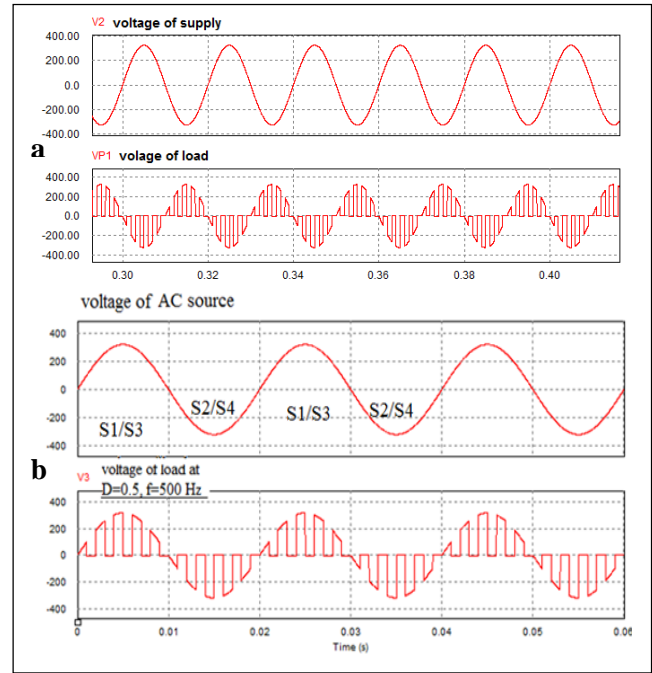

Fig. 2. Simulated diagrams of modulated load voltage Dcon=D$_R$=0.5, U1m=325 V, 50 Hz; fM=500 Hz . a – an concurrent waves of supply and fundamental harmonic of load voltage; b – reverse waves of supply and load fundamental waves.

Table II   Comparison of experimentally obtained and calculated results.

Not changed polarities	Reverse polarities	
Amplitude voltage of the fundamental wave, V	Amplitude voltage of the fundamental,	RMs values of fundamental for concurrent voltages for reverse waves
162.7 V ; experimental 162.1 V	-162.7V; experimental – 162.1 V	Calcul. 114.0 V, experimental 114.5 V Voltmeter – 162.367

The modulated voltage has a poor indicator of the quality – the THD (total harmonic distortion) factor, i.e., it contains many higher harmonics (see Fig. 3).

Fundamental harmonic of current developed from such voltages currents can be described as $i_1 = D \cdot i_{ld} \cdot sin \omega t$, the effective RMS value of such a current is defined as $I_{1rms} = D.I_{ld}/\sqrt{2}$, and the apparent power of the power supply is defined as

$$S_1 = U_{1rms} \cdot I_{1rms} = \frac{U_{1m} \cdot DU_{1m}}{\sqrt{2}Z_{ld}\sqrt{2}} = \frac{DU_{1m}^2}{2Z_{ld}} \qquad (2)$$

Real power is defined as $P_{ld} = I_{ld}^2 \cdot R$ and if there are no other devices with real power in the circuit, then the power factor will be defined as:

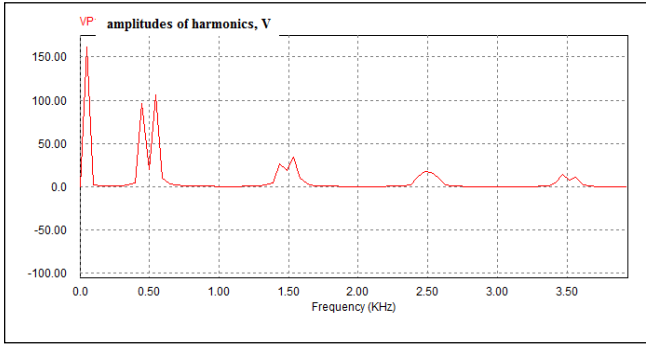$$\Psi = \frac{p_1}{S_1} = \frac{DU_1R}{Z_{ld}} \qquad (3)$$

Fig. 3. Diagram of amplitudes of higher harmonics in content of modulated load voltage.

Fig. 4. Schematic for realization of harmonic filter for modulated load voltage.

3 Filtering modulated load voltage

To obtain a sinusoidal alternating current under specific load corresponding to the fundamental harmonic voltage, it is necessary to suppress all other harmonic orders (see Fig. 3). In parallel to the load, capacitor C is connected (Fig. 4), but in series with the circuit the inductor L is introduced. If the both elements are selected correctly, the load voltage is slightly different from the sinusoid with the mains frequency $\omega = 2\pi f$, where f is the frequency of AC voltage supply source. THD indicator for the load voltage becomes closer to the zero value. Modulated voltage uD, RMS value of which is DU_1 is not sinusoidal at all, but in the vector diagram it can be replaced by the voltage vector of the fundamental harmonic, and as consequently the load voltage UC can be determined from the vector expression $\overline{U_D} = \overline{U_C} + \overline{U_L}$ which is assumed to be sinusoidal, and calculated from the specified equation as:

$$\overline{U_C} = \overline{U_D} - \overline{U_L}. \qquad (4)$$

The inductor L current can be calculated by considering the capacitor and load currents data (see vector diagram for voltage vectors and currents in the scheme Fig.5).

$$I_L^2 = I_C^2 + I_R^2 = \frac{U_C^2 \cdot \omega^2 C^2}{1} + \frac{U_C^2}{R^2} = U_C^2(\frac{1}{R^2} + C^2\omega^2). \qquad (5)$$

In this case, the inductor current vector leads the load voltage vector by the angle φ, which can be calculated by:

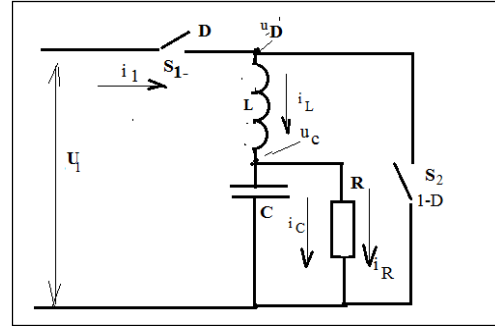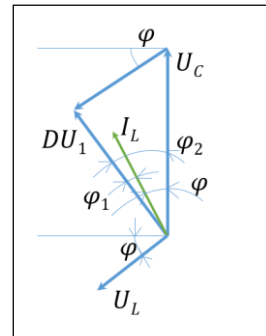$$\varphi = actg\ \omega RC. \qquad (6)$$

Fig. 5. Vector diagram for voltages and currents in the scheme of filter.

The inductor voltage will be defined as:

$$U_L = I_L \omega L = a \cdot U_c \cdot \omega L. \qquad (7)$$

where $a = \sqrt{\frac{R^2\omega^2C^2+1}{R^2}}$ factor represents the relation between RMS current of an inductor and RMS voltage of load circuit, and the vector of this voltage is ahead of the current I_L vector by 90 degrees. The total sum of both vectors is equal to the RMS value of the modulated $\overline{U_D} = \overline{U_C} + \overline{U_L}$.

By substituting the values of the expressions, it is obtained:

$$U_D^2 = [U_C - U_L \cos(90 - \varphi)]^2$$
$$+ [U_L \sin(90 - \varphi)]^2$$
$$= U_C^2 - 2U_{C.}aU_C\omega L cos(90 - \varphi)$$
$$+ U_C^2 a^2 \omega^2 L^2 cos^2(90 - \varphi)$$
$$+ a^2\omega^2 L^2 U_C^2 sin^2(90 - \varphi)$$
$$= U_C^2\big(1 + a^2\omega^2 L^2$$
$$- 2a\omega L cos(90 - \varphi)\big) = U_D^2$$

or $\frac{U_D^2}{U_C^2} = 1 + a^2\omega^2 L^2 - 2\omega a L cos(90 - \varphi)$.

$$\frac{U_D}{\sqrt{1+a^2\omega^2L^2-2a\omega Lcos(90-\varphi)}} = U_C. \qquad (8)$$

Denoting the expression under the root as b, yields:

$$U_C = \frac{U_D}{b}.$$

4 Regressive estimation of filtering system parameters on quality of the system

Considering that, the angle $\varphi = arc\ tg\ (\omega RC)$, it is possible to analyze the influence of each parameter on the value of the load voltage U_C. The best approach is to use the regressive expression method – for example getting an algebraic expression $X = X_0 + aX_1^* + bX_2^* + cX_3^*$ ...

where X is the present value of parameter X_0 mean value of the entire family of experimental results, X_1^*, X_2^* ,... - normalized values of influence parameters 1,2,3…; a, b, c…,indicators of influence of each parameter .

If, for example, the capacitance of a capacitor is considered in the range between 50 µF to 200 µF and the wired load resistance R value is between 1 ohm to 100 ohm, then at an angular frequency of ω=314 1/s (50 Hz), the following table of angle φ values calculated by the formula should be considered.

Table III   φ values calculated by the formula.

R*	C*	φexp. Gr	φform. Gr
-1	-1	0,9	-4,3
-1	+1	3,6	8,8
+1	+1	81	75,8
+1	-1	57,5	62,7

If the ratios are described as

$$\varphi = \varphi_0 + AR^* + BC^*, \qquad (9)$$

where $\varphi_0 = \frac{\sum_i^N \varphi_i}{N}$ – the average value of the calculation results, the indicator A takes into account the influence of the resistor parameter on the angle value

$$A = \frac{\sum_1^N R_i^* \varphi_i}{N} \qquad (10)$$

and the indicator B of the influence of the C parameter on the angle.

$$B = \frac{\sum_1^N C^* \varphi_i}{N}. \qquad (11)$$

As a result of indicator calculations φ=35.75+35.5R*+6.55C*, where $\varphi_0 = 35.75\ gr$, $A = 35.5\ gr$ $B = 6.55\ gr$, diagram of factors influencing the angle φ dependence in

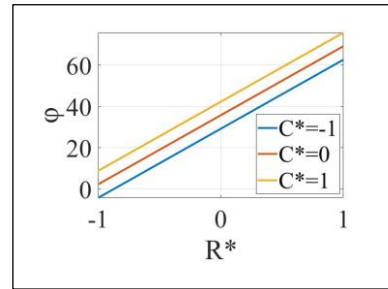accordance with the regression formula obtained is presented in Fig.6.

Fig. 6. Diagram of factors influencing the angle φ in accordance with the regression formula obtained

Having carried out calculations using the obtained regression formula, we obtain the values with index *form*, which are also given in table IV. As you can see, the values calculated by the obtained formula for the reference points coincide quite well with those calculated by the exact expression.

The dependence of the inductor current I_L on the load voltage U_C at different parameters of the elements R and C conducting research on the indicator a:

$$a = \sqrt{\frac{1}{R^2} + \omega^2 C^2}, \qquad (12)$$

Carrying out similar actions as in the first case, we create a table of indicators a found about the expression as:

Table IV   Table of indicators *a*

R*	C*	aexp.	aform.
-1	-1	1	0.988
-1	+1	1	1.01
+1	+1	0.064	0.0513
+1	-1	0.0186	0.0287

Hence it is expressed as

$$a = 0.52 - 0.48R^* + 0.0113C^* \qquad (13)$$

As a matter of fact, in this case the coincidence of the results in terms of the analytical expression and the statistical one is quite close, too. Knowing the indicator a, the inductor current is calculated as:

$$I_L = aU_C \qquad (14)$$

As it can be observed, if, with other parameters unchanged, a increases, then the inductor current also grows. In this case, the more R*, the smaller becomes a (see Fig.7), and at R* max becomes zero. Accordingly, the inductor current magnitude is also small.
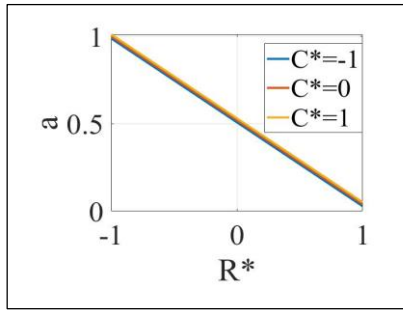
Fig. 7. Diagram of dependence an indicator *a* on parameters of filter load circuit according the regression formula developed.

Similarly, it is possible to investigate changes in the load voltage, but already depending on the three parameters of the elements R, L, C (see the table to establish the values of *b* for various parameters), The inductance of the inductor is considered in the zone from 1 mH to 20 mH.

Table V   Values of *b* for various parameters.

R*	L*	C*	b	bform
-1	-1	-1	1.043	8.276
-1	-1	+1	1.06	8.364
-1	+1	-1	31.4	23.536
-1	+1	+1	31.35	23.624
+1	-1	-1	0.995	-6.524
+1	+1	-1	0.597	8.736
+1	+1	+1	1.024	8.824
+1	-1	+1	0.98	-6.436

From the data table we can get the regression expression $b = 8.55 - 7.4R^* + 7.63L^* + 0.044C^*$ which is illustrated in the Fig.8.
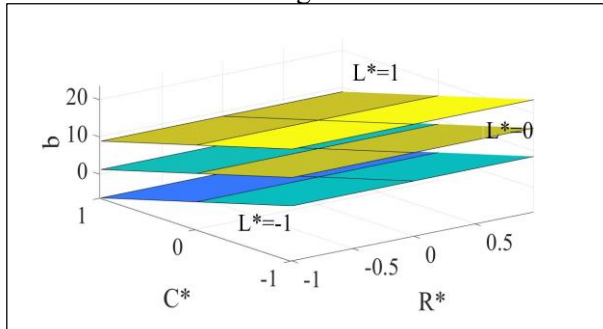

Fig. 8. Dependence diagram of load voltage level indicator **b** on parameters of filter elements by a developed regression formula.

We remind that the effective value of the load voltage is defined as the division of the effective value of the fundamental wave of the modulated voltage DU_1 by the indicator **b**, which depends on the parameters of the three elements $U_c = \frac{DU_1}{b}$.

Considering the graph of the dependence of **b** on the parameters, it is evident that there is a strong dependence of the magnitude of the inductance of the inductor L. The larger the L, the larger the indicator **b** also. It should be noted that the indicators of the

influence of R and L have opposite signs with equal absolute values. This means that with an increase in R, in order to stabilize the value of b and the level of load voltage, the value of L should be increased, i.e. the inductor should be characterized by the nonlinearity of the inductance depending on the current – at lower currents through the inductor the inductance of the winding should be higher than in higher currents.

The values of the angles between different currents and voltages of the node are very important. One of the most important is the angle φ_1 between the current I_L and the modulated voltage vector U_D , which can be called the input shift angle of the node vectors. Using the similar method as previous) it is possible from table of calculated data (see the table by exact expression) express angle φ_2 between vector of modulated supply voltage and load voltage

$$\varphi_2 = 58.97 + 5.12R^* + 50L^* - 4.626C^* \quad (15)$$

Table VI   Calculated data (see the table by exact expression) express angle φ2 between vector of modulated supply voltage and load voltage.

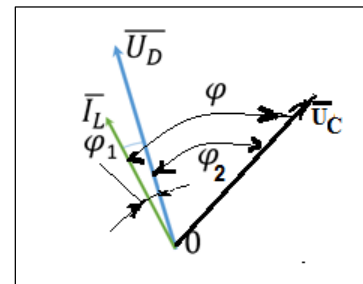| R*	L*	C*	φ_2	φ_{2form}
-1	-1	-1	17.74	8.47
-1	-1	+1	17.73	-0.776
-1	+1	-1	88.17	108.47
-1	+1	+1	91.78	90.236
+1	-1	-1	0.186	18.71
+1	-1	+1	0.182	9.46
+1	+1	-1	148.3	118.7
+1	+1	+1	107.7	109

Fig. 9. Phasor diagram of load node.

The entry angle is usually leading (i.e., the current vector leads the modulated voltage vector, see fig. 9). Again, with increasing inductance, the angle increases in magnitude.

For some parameters of the elements, the angle is close to zero, i.e. the node works as an active one, however, with others, the lead can reach 90 and more degrees $\varphi_1 > 90°$ in the leading direction. The expression for the φ_1 also can be easily visualized. If both angles ϕ and ϕ1 are known, then the angle between the vector of the modulated voltage and the vector of the load voltage is determined as:

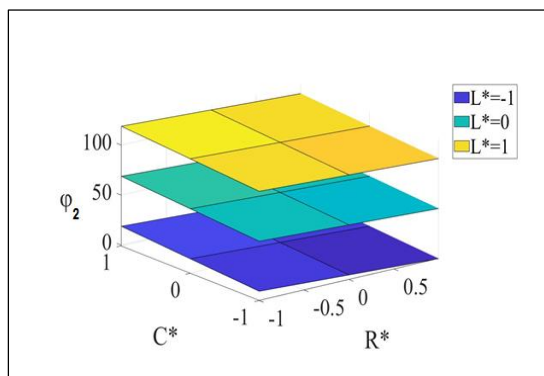$$\varphi_2 = \varphi - \varphi_1. \qquad (16)$$

Fig. 10. Diagram of parameters influence on the angle between vector of modulated supply voltage and load voltage in accordance with the developed regression formula.

By examining the considered relations, one can get a general idea of the nature of the influence of the parameters of the elements. Figure 10 shows some of the obtained diagrams of currents and voltages of the elements of the filtering system at C = 100 μF, R = 10 Ω, L = 5 mH. Normalized parameters of elements in the case are $C^* = -1 + \frac{2(100-50)\mu F}{(200-50)\mu F} = -0.333$ and $R^* = -1 + \frac{2(10-1)\Omega}{99\Omega} = -0.636$.

To check the correctness of the expressions obtained for the modulated voltage filter, a calculation was carried out by expressions obtained and a comparison of the calculation results with the experimentally obtained data (based on a computer model). The following values of the parameters of the voltage modulation system were used: RMS value of supply AC voltage U_1=230 V, duty ratio for modulation D=0.5, reduced resistance of the load R=10Ω, inductance of the filter coil L=5 mH, capacitance for load resistance C=100 μF.

The results of the comparison are summarized in a table, which shows the calculated and experimentally obtained values of the RMS of the modulated voltage $U_{D(1)}$, the RMS voltage on the plates of the load capacitor Uc, the effective value of the inductor current I_L, the values of the ratio factors b and a, as well as the values of the angles of the phase shift ϕ between the I_L and U_C, the angle ϕ_2 of the shift between the voltage vectors $U_{D(1)}$ and the load one U_C, as well as the phase shift ϕ_1 between the vectors I_L and the vector of the modulated voltage $U_{D(1)}$.

Table VII. Comparison between experimental results and calculated results

UD(1), V	UC V	IL , A	φ, deg	φ2 deg	φ1 deg
Exp calcul	Exp calcul	Exp calcul	Exper calcul	Exper calcul	Exper calcul
114.5 115	119.16 119.34 b=0.96 bcalc=0.9636	12.53 12.51 aexp=0.105 acalc=0.1048	16.63 17.43	9.03 9.38	7.6 8.05

As you can see, the coincidence of the calculated and experimentally obtained results is even very good, which confirms the possibility of calculating and analyzing complex modulated alternating current systems using vector methods, representing vectors with effective values of currents and voltages based on the generated by modulations new fundamental waves of currents and voltages. Evaluation of the accuracy of the obtained regression expressions shows that since they were obtained for a wide range of changes in the input parameters of the system elements, the accuracy is often low, especially when using the obtained regression expressions for calculation of the ratios of parameters, i.e., a, b, ϕ, ϕ_2. So, for example, using the data adopted in the construction of the table ϕ_2= 9.03 deg, but according to the regression expression this parameter is 47.8 deg .. However, the regression expressions give a very good idea of the influence of individual parameters on the overall result.

5 Technical example of using unipolar switch modulation

As a technical example, consider the use of three unipolar modulated switch AC regulators for smooth start-up of a three-phase induction electric motor with a cage rotor (three-phase asynchronous squirrel-cage motor) from a network of three phase (phase-neutral) voltages A_1-N_1, B_1-N_1, C_1-N_1 with a smooth increase the RMS value of these voltages in respect to the phases of an electric motor during starting the motor. The induction motor in this system also has a neutral point N_M (fig. 11).

In each of the three phases of the supply network and the motor, two oppositely switched electronic switches of alternating current conductivity are switched on: when S1 conducts alternating current, then S2 does not conduct current at all (locked) and vice versa, when S1 is locked, the switch S2 conducts alternating current, thereby creating a zero voltage interval for the phase of motor. If both switches switch at a relatively high frequency (about 100 times higher than the frequency of the mains supply voltage) and the S1-on state in the switching period

is active with a relative duration D (duty ratio), then the S2-on interval in the switching period T_M has a relative duration of 1-D. In this case, the fundamental harmonic of the phase (neutral-phase) voltage of the motor is represented by a wave
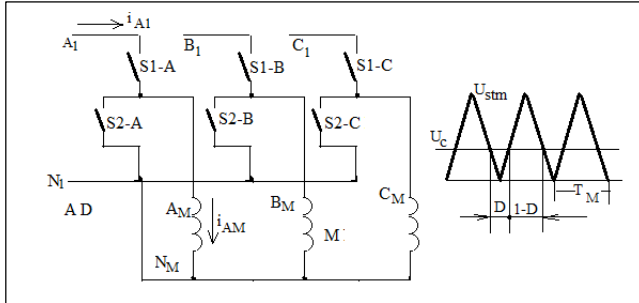

Fig. 11. The induction motor connection.

$$u_{Mph(1)} = D \cdot U_{phm} \sin \omega t \qquad (17)$$

where U_{phm} is the amplitude of the voltage supply phase-neutral, $\omega = 2\pi f_1$ is the angular frequency of the supplying alternating voltage. The effective (RMS) voltage of the fundamental wave of the phase voltage of the motor is defined as

$$U_{Mph(1)} = \frac{D U_{phm}}{\sqrt{2}} \qquad (18)$$

If for a soft start it is supposed to linearly increase this effective voltage, then the starting process is characterized by a linear increase in time in the indicator D from the minimum value D = 0 corresponding to the minimum necessary RMS voltage value to the D = 1 (if the nominal values of the network and the motor voltages are equal).

Change of D can be carried out by fixing the interception points of a unipolar saw-shaped voltage u_{st} with a modulation frequency = $1/T_M$ with slowly variable control voltage U_C over the modulation period. Signal for unlocking the switches S1 in all three phases is supplied when the control voltage exceeds the instantaneous values of the saw-tooth voltage with an amplitude U_{stm} , i.e. the relative duration of the switched-on S1 (Duty ratio) is expressed as

$$t_D = \frac{U_C}{U_{stm}} \qquad (19)$$

and the relative duration of switching on the switches S2 is as

$$t_{1-D} = 1 - \frac{U_C}{U_{stm}} \qquad (20)$$

Modeling of this system is carried out at a switch modulation frequency of 5 kHz with an asynchronous

electric motor of the resistance of the stator and rotor windings (reduced to the stator), respectively, 0.294 ohm and 0.156 ohm with the inductance of these windings 1.39 mH and 0.74 mH, magnetizing inductance 41 mH, number of poles 6 and moment of inertia 0.4 kg.m². The motor parameters correspond to approximately 15-20 kW rated power. Diagrams of the instantaneous current of the motor, power supply, corrected control voltage and speed of the motor shaft are shown in Fig. 12.
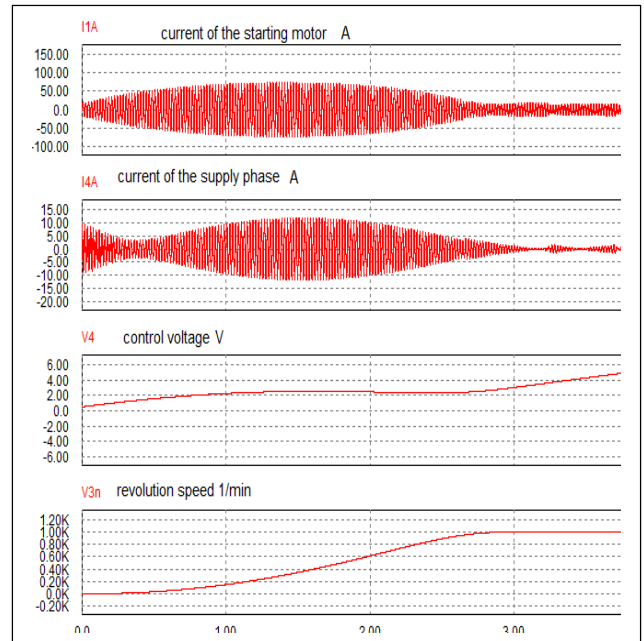

Fig. 12. Diagrams of the instantaneous current of the motor, power supply, corrected control voltage and speed of the motor shaft.

The control voltage was corrected with the deduction of the component approximately proportional to the current amplitude of the motor from the linearly increasing control voltage, which allows better linearization of the character of the motor speed rise at starting. To ensure a smooth and linear increase in the speed of the motor during start-up, for any peculiarities of the influence of the motor load, it is necessary to use a significantly advanced start-up control with the control of the magnetic field of the motor during start-up.

Figure 13 shows the experimentally taken diagrams of currents of all three phases of an asynchronous electric motor in the middle of a smooth start of an electric motor in the proposed soft start system. As you can see, the waves of currents are close to sinusoidal, which is a consequence of the generation of fundamental waves of voltage of the phases of the motor by modulated switches.
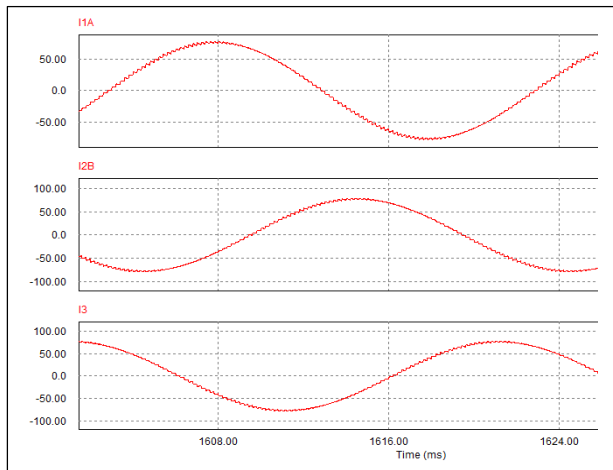
Fig. 13. Experimentally taken diagrams of currents of all three phases of an asynchronous electric motor.
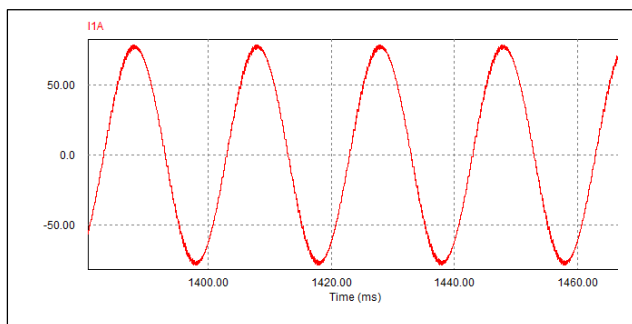

Fig. 14. Output voltage.

To obtain sinusoidal diagrams of the power supply currents in phases of the supplying alternating current, it is necessary to turn on the L-C filter modulated by the current. In the case here L=1 mH/phase but capacitance is 50 μF/ phase. The filter turns out to be quite light, since the modulation frequency during the start-up process is taken quite high at the level of 5 kHz.

6 Conclusion

Using the mentioned approach, a vector diagram for a complex circuit has been created, on the basis of which the main parameters of such a circuit - voltage values on the load capacitor, inductor current RMS values, shift angles between different voltages and currents, etc. calculation.

The results obtained in terms of expressions coincide very well with those obtained in practical models, which prove the validity of the approach.

The value of the filter voltage is sensitive to an increase in the load on the circuit connected to the capacitor, but as the statistical processing of the calculations for a sufficiently wide range of element parameters shows, this decrease can be compensated by a decrease in inductance with a nonlinear inductance.

References:

[1] J. Kaniewski, P. Szczesniak, M. Jarnut and G. Benysek , "Hybrid Voltage Sag/Swell Compensators: A Review of Hybrid AC/AC Converters", *IEEE Industrial Electronics Magazine, vol. 9, issue 4, pp. 37-48, Dec.* 2015.

[2] J. M. Flores-Arias, A. Moreno-Munoz, R. Real-Calvo, J. R. Sanchez, "Transformerless power line voltage conditioner and regulator based on CA PWM Chopper", presented at 2010 IEEE International Symposium on Industrial Electronics, Bari, Italy, July 4-7, 2010.

[3] O. C. Montero-Hernhdez, P. N. Enjeti, "Application of a Boost AC-AC Converter to Compensate for Voltage Sags in Electric Power Distribution Systems", in *Proc. 31st Annual Power Electronics Specialists Conf.*, 2000. pp. 470-476.

[4] Dong-Myung Lee, T. G. Habetler, R. G. Harley, J. Rostron and T. Keister, "A voltage sag supporter utilizing a PWM-switched autotransformer," *2004 IEEE 35th Annual Power Electronics Specialists Conference (IEEE Cat. No.04CH37551)*, Aachen, Germany, 2004, pp. 4244-4250 Vol.6.

[5] I. Rankis, M. Prieditis and G. Stana, "Investigation of dirrect AC-AC BUCK converter with series injection transformer," *2018 IEEE 59th International Scientific Conference on Power and Electrical Engineering of Riga Technical University (RTUCON)*, Riga, Latvia, 2018, pp. 1-6.

[6] A. Purwar, D. Joshi and M. S. Dasgupta, "Smart control of electric lamp using artificial intelligence based controller," *2015 Annual IEEE India Conference (INDICON)*, 2015, pp. 1-5, doi: 10.1109/INDICON.2015.7443228.

[7] A. L. Neri and A. C. C. Lyra, "Starting Control Using Angle Adjustment of the Double Dimmer Supply Method for Single-Phase Induction Motor," *2006 12th International Power Electronics and Motion Control Conference*, 2006, pp. 979-983, doi: 10.1109/EPEPEMC.2006.4778527.

[8] S. Tunyasrirut, B. Wangsilabatra and T. Suksri, "Phase control thyristor based soft-starter for a grid connected induction generator for wind turbine system," ICCAS *2010*, 2010, pp. 529-534, doi: 10.1109/ICCAS.2010.5669944.

[9] S. Gautam, A. K. Yadav and R. Gupta, "AC/DC/AC converter based on parallel AC/DC and cascaded multilevel DC/AC converter," *2012 Students Conference on Engineering and Systems*, 2012, pp. 1-6, doi: 10.1109/SCES.2012.6199078.

[10] C. Benboujema, A. Schellmanns, N. Batut, J. B. Quoirin and L. Ventura, "Low losses bidirectional switch for AC mains," *2009 13th European Conference on Power Electronics and Applications*, 2009, pp. 1-10.

[11] H. Takano, T. Domoto, J. Takahashi and M. Nakaoka, "Auxiliary resonant commutated soft-switching inverter with bidirectional active switches and voltage clamping diodes," *Conference Record of the 2001 IEEE Industry Applications Conference. 36th IAS Annual Meeting (Cat. No.01CH37248)*, 2001, pp. 1441-1446 vol.3, doi: 10.1109/IAS.2001.955725.

[12] I. Rankis and M. Prieditis, "Properties of the AC/AC buck-boost converter," *2017 IEEE 58th International Scientific Conference on Power and Electrical Engineering of Riga Technical University (RTUCON)*, 2017, pp. 1-6, doi: 10.1109/RTUCON.2017.8124777.

[13] M. Zhuri, "Power system analysis: The case of Albania", International Journal of Innovative Technology and Interdisciplinary Sciences - Volume 3, Issue 4, 2020, https://doi.org/10.15157/IJITIS.2020.3.4.50 1-512, ISSN 2613-7305.

[14] A. Romanovs, I. Pichkalov, E. Sabanovic and J. Skirelis, "Industry 4.0: Methodologies, Tools and Applications," *2019 Open Conference of Electrical, Electronic and Information Sciences (eStream)*, 2019, pp. 1-4, doi: 10.1109/eStream.2019.8732150.

[15] A. Romanovs et al., "State of the Art in Cybersecurity and Smart Grid Education," IEEE EUROCON 2021 - 19th International Conference on Smart Technologies, 2021, pp. 571-576, doi: 10.1109/EUROCON52738.2021.9535627.